Celestial Mech Dyn Astr (2007) 97:87–100
DOI 10.1007/s10569-006-9053-6

ORIGINAL ARTICLE

A note on weak stability boundaries

F. García · G. Gómez

Received: 13 March 2006 / Revised: 4 September 2006 /
Accepted: 9 October 2006 / Published online: 8 December 2006

Abstract This paper is devoted to clarify the algorithmic definition of the weak stability boundary in the framework of the planar Restricted Three Body Problem. The role of the invariant hyperbolic manifolds associated to the central manifolds of the libration points L_1 and L_2, as boundary of the weak stability region, is shown.

Keywords Weak stability boundaries · Invariant manifolds · Libration points

1 Introduction

The *weak stability boundary* (WSB) is a concept mainly developed after Belbruno (1987) and the rescue of the Hiten spacecraft (see Belbruno and Miller 1990). A careful look to the transfer trajectory of this spacecraft from the Earth to the Moon (see Koon et al. 2000, 2001) shows that first visited a neighbourhood of the collinear libration point L_1 of the Earth–Sun system, afterwards went to the vicinity of the L_2 point of the Earth–Moon system, and finally reached the Moon.

Transfers similar to the one described above are named *WSB transfers*; they require a large transfer time (between 60 and 100 days) but a small Δv (saving up to 150 m/s with respect to a Hohmann transfer) since they eliminate the hyperbolic excess velocity at lunar periapsis upon arrival, for this reason, they are also called *low energy transfers*. Furthermore, they use the dynamics of the problem in a more natural way than the Hohmann transfers do.

F. García · G. Gómez (✉)
Departament Matemàtica Aplicada i Anàlisi,
Universitat de Barcelona,
Gran Via 585,
Barcelona 08007, Spain
e-mail: gerard@maia.ub.es

F. García
e-mail: ferrangarcia@ub.edu

There is a large number of papers dealing with WSB transfers going from the Earth to the Moon (see, for instance, Belbruno 1994; Belbruno et al. 1997; Belbruno and Carrico 2000; Bello et al. 2000; Belbruno et al. 1997; Circi and Teofilato 2001; Yagasaki 2004a,b). The most well known method to find these kind of transfers (Miller and Belbruno 1991) starts from a low Lunar orbit and, after giving a Δv, integrates backwards in time until a point within the *WSB region* is reached. A second integration starts from a parking orbit around the Earth and, after giving a Δv, integrates forward in time. Both integrations are altered such that the final positions of the transfer match. In order to minimise the total Δv, optimisation methods of different kinds are used. In these papers the WSB region is just defined as a region approximately 1.5 million kilometres away from the Earth in the Sun–Earth direction. It must be remarked that at this distance is where the libration point orbits around L_1 and L_2 points of the Sun–Earth system are.

The WSB region (also named *fuzzy boundary region*) has not got a precise definition, at least in the usual mathematical sense of the word. Some definitions that can be found in the literature, aside from the one given above, are: "*a generalisation of the Lagrange points and a complicated region surrounding the Moon*" (Belbruno and Miller 1990), "*a region in phase space supporting a special type of chaotic motion for special choices of elliptic initial conditions with respect* m_2" (Belbruno 2002), "*a transition region between the gravitational capture and escape from the Moon in the phase space*" (Yagasaki 2004a), …

According to Belbruno (2004), the WSB can be defined in the framework of the planar Restricted Three Body Problem (RTBP) in the following way: let $(\mathbf{x},\dot{\mathbf{x}}) \in \mathbb{R}^4$ be the state of the infinitesimal particle m in barycentric rotating coordinates. Consider the sets

$$\Sigma = \{(\mathbf{x},\dot{\mathbf{x}}) \mid h_K(\mathbf{x},\dot{\mathbf{x}}) \leq 0\}, \quad \sigma = \{(\mathbf{x},\dot{\mathbf{x}}) \mid \dot{r}_2 = 0\},$$

where h_K denotes the Keplerian energy of m with respect the small primary m_2 and r_2 the distance from m to m_2. Recall that the energy for the Kepler problem is given by (see Pollard 1996)

$$2|h_K| = \frac{\mu}{a}, \tag{1}$$

where a is the semi-major axis of the orbit.

Then, if $J(\mathbf{x},\dot{\mathbf{x}})$ is the Jacobi integral of the RTBP, the weak stability boundary W associated to a given value C of the Jacobi constant is

$$W = J^{-1}(C) \cap \Sigma \cap \sigma. \tag{2}$$

There is also an algorithmic definition of the WSB (see Belbruno 2002,2004). Consider a radial segment, $l(\theta)$ departing from the small primary m_2 and making an angle θ with the x-axis. Take trajectories for the infinitesimal body, m, starting on $l(\theta)$ which satisfy

1. The particle m starts its motion at the periapsis of an osculating ellipse around m_2, at a certain point on $l(\theta)$. If r_2 denotes the distance between m and m_2 at this point, then

$$r_2 = a(1-e),$$

where a and e are the semi-major axis and eccentricity of the ellipse.

2. The initial velocity vector of the trajectory is perpendicular to the radial segment $l(\theta)$.
3. The initial two-body Kepler energy, h_K, of m with respect to m_2 is negative. The value of h_K, computed at the periapsis, is given by

$$h_K = \frac{\mu}{2}\frac{e-1}{r_2}, \tag{3}$$

so, clearly, if $e \in [0,1)$ then $h_K < 0$.
4. The eccentricity of the initial two-body Keplerian motion is held fixed along $l(\theta)$. According to (3), this condition is equivalent to fix the value of h_K.

For the motions with the above initial conditions, the following definition of stability and instability is given (see Belbruno 2002, 2004):

Definition 1.1 The motion of a particle is said to be *stable* about m_2 if after leaving $l(\theta)$ it makes a full cycle about m_2 without going around m_1 and returns to $l(\theta)$ at a point with negative Kepler energy with respect to m_2. Of course, the motion will be *unstable* if the above condition is not fulfilled.

In the above mentioned papers, it is claimed (without giving any proof or numerical evidence) that as the initial conditions vary along $l(\theta)$, there is a finite distance $r^*(\theta, e)$, depending on the polar angle θ and the eccentricity e of the initial osculating ellipse, such that:

– If $r_2 < r^*$, the motion is stable.
– If $r_2 > r^*$, the motion is unstable.

Furthermore, $r^*(\theta, e)$ is a smooth function of θ and e which defines the WSB

$$\mathcal{W} = \left\{ r^*(\theta, e) \mid \theta \in [0, 2\pi], e \in [0,1) \right\}.$$

This algorithmic definition is not accurate in the following point:

– The requirements on the initial conditions fix the modulus of the velocity and its direction, but not the sense. So, for a fixed position on $l(\theta)$, there are two different initial velocities, fulfilling the four restrictions, which can produce orbits with different stability behaviour. These two possibilities correspond to the two components of the WSB mentioned in Belbruno (2004).

On the other hand:

– It is not clear that, for fixed values of θ and e, there is a finite distance $r^*(\theta, e)$ defining the boundary of the stable and unstable orbits. As will be shown in the next section, along $l(\theta)$ there are several transitions from stability to instability. In fact, for a fixed value of θ, the set of stable points recalls a Cantor set.
– Also, some maximum time interval must be fixed for the numerical integration. In our computations, we have taken it equal to 80 adimensional time-units. It may happen and, in fact it does, that after this time interval the orbit departing from l does not cross again this segment, in this case (which certainly is not very frequent) we have considered the orbit as unstable.

The suitable setting for the WSB-transfers is the restricted four body problem, as follows from the kind of trajectories associated to the low energy transfers and as it is

also established in Belbruno (1994). This last paper has a heuristic explanation, using invariant manifolds and Hill's regions, about how a ballistic capture by the Moon can take place, but it has not any numerical computation supporting the claims. Nevertheless, introduces for the first time, to our knowledge, a model for the restricted four-body problem consisting in two different restricted three body problems which has been extensively used in Koon et al. (2000, 2001) to explore more systematically some of these kind of transfers. These transfer orbits will be not considered in this paper.

The goals of the present paper are:

1. Using the algorithmic definition of the WSB previously mentioned, compute the boundary between the stable/unstable regions around m_2 for different values of the eccentricity e and using the two different determinations of the velocity.
2. Give a very rough estimate of the stable/unstable regions around the small primary.
3. Compute the stable and unstable invariant manifolds associated to orbits around the collinear Lagrangian points, in order to see the connection between those manifolds and the stable/unstable regions.

2 Computation of stable motions about m_2

As it has been said, the framework in which the WSB is defined is the Restricted Three Body Problem, which describes the motion of a massless particle in the gravitational force field created by two main bodies—primaries—in Keplerian circular motion around their centre of mass.

If m_1 and m_2 are the masses of the primaries, we will use for the mass ratio its usual definition $\mu = m_1/(m_1 + m_2)$ so, in the sinodical barycentric reference system and with the usual units of longitude, mass and time, the equations of motion are (see Szebehely 1967)

$$\ddot{x} - 2\dot{y} = \frac{\partial \Omega}{\partial x}, \qquad \ddot{y} + 2\dot{x} = \frac{\partial \Omega}{\partial y}, \tag{4}$$

with

$$\Omega(x, y) = \frac{1}{2}(x^2 + y^2) + \frac{1-\mu}{r_1} + \frac{\mu}{r_2} + \frac{1}{2}\mu(1-\mu),$$

and $r_1^2 = (x-\mu)^2 + y^2$, $r_2^2 = (x+1-\mu)^2 + y^2$. System (4) has the well known Jacobi's first integral

$$J(\mathbf{x}, \dot{\mathbf{x}}) = 2\Omega(x, y) - (\dot{x}^2 + \dot{y}^2) = C, \tag{5}$$

where C is the so called Jacobi constant.

For all the computations that follow, the value of the mass parameter that has been used is $\mu = 0.0121506683$, corresponding to the one of the Earth–Moon system.

According to Definition 1.1 for the WSB, to determine the stable/unstable regions around m_2, Eq. 4 must be integrated taking initial conditions along the radial segment $l(\theta)$ and with the initial velocity vector perpendicular to it. In this way, for any point along $l(\theta)$ there are two different initial conditions, that have been called with positive and negative velocity, respectively. In order to fulfil the other requirements, it is easily verified that in the barycentric sinodical reference system and starting at a distance r_2 from m_2, the initial conditions must be:

– Initial conditions with positive velocity (osculating retrograde motions about m_2)

$$x = -1 + \mu + r_2 \cos\theta, \quad y = r_2 \sin\theta,$$
$$\dot{x} = r_2 \sin\theta - v \sin\theta, \quad \dot{y} = -r_2 \cos\theta + v \cos\theta.$$

– Initial conditions with negative velocity (osculating direct motions about m_2)

$$x = -1 + \mu + r_2 \cos\theta, \quad y = r_2 \sin\theta,$$
$$\dot{x} = r_2 \sin\theta + v \sin\theta, \quad \dot{y} = -r_2 \cos\theta - v \cos\theta.$$

In both cases, the modulus of the initial sidereal velocity of the infinitesimal particle is equal to v. Recall that, if the larger primary m_1 is removed, these initial conditions must correspond to elliptic Keplerian orbits around m_2 starting at the pericenter so, for a certain value of the eccentricity, the value of v will be given by

$$v^2 = \mu \left(\frac{2}{r_2} - \frac{1}{a} \right) = \frac{\mu(1+e)}{r_2}.$$

For fixed values of the eccentricity e and the angle θ, we have looked for all the possible values of the distance r^* along l for which there is a change of the stability properties of the orbit (according to Definition 1.1). In this way, we are able to find a finite number of points (up to a certain precision) $r_1^* = 0, r_2^*, \ldots, r_{2n}^*$ such that if $r_2 \in [r_1^*, r_2^*] \bigcup [r_3^*, r_4^*] \bigcup \ldots \bigcup [r_{2n-1}^*, r_{2n}^*]$ then motion is stable and otherwise unstable. The number of points r_i^* as well as their values depend, of course, on e, θ and the precision of the computations.

According to these remarks, we can extend the algorithmic definition of the WSB as the boundary $\partial\overline{\mathcal{W}}$ where

$$\overline{\mathcal{W}} = \left\{ [r_{2k-1}^*(\theta, e), r_{2k}^*(\theta, e)],\ k = 1, \ldots, n\,;\ \theta \in [0, 2\pi], e \in [0, 1) \right\}.$$

We have numerically computed the set $\overline{\mathcal{W}}$ for different values of the initial eccentricity $e = 0, 0.05, 0.1, \ldots, 0.95, 0.99$, discretising the angular parameter θ using 1000 equidistant values in $[0, 2\pi]$ and the distance r_2 along l with equidistant increments of $5 \cdot 10^{-3}$ adimensional units. The maximum value explored for r_2 has been 1.7 adimensional units; for this value of r_2 almost all the orbits explored are unstable.

The integration of the RTBP equations of motion has been done using a Runge–Kutta–Felhberg 7–8 method with automatic step size control and local truncation error less than 10^{-14}. The equations of motion have been regularised, using Levi–Civita regularisation (Szebehely 1967), when the motion of the small particle is inside a disc of radius 10^{-2} around any primary.

Figures 1 and 2 display the behaviour of the set $\overline{\mathcal{W}}$, for different values of the eccentricity, using initial conditions with positive and negative velocity, respectively. As is clearly seen, the structure of $\overline{\mathcal{W}}$ is not as simple as it was claimed in Belbruno (2002, 2004), in the sense that for any value of the angle θ there is not a single value of r^* defining the boundary of the stable region. The geometry of $\overline{\mathcal{W}}$ becomes more complicated as the value of e increases and is rather different when the positive of the negative velocities are used.

We have done a simple numerical experiment to test the robustness of these stability definition as a function of the number of intersections of the trajectory of the infinitesimal particle m with the segment l, this is, the number of cycles that the particle m makes around the small primary fulfiling the conditions of Definition 1.1. Instead of using the first intersection with l, in order to establish the stability/instability of

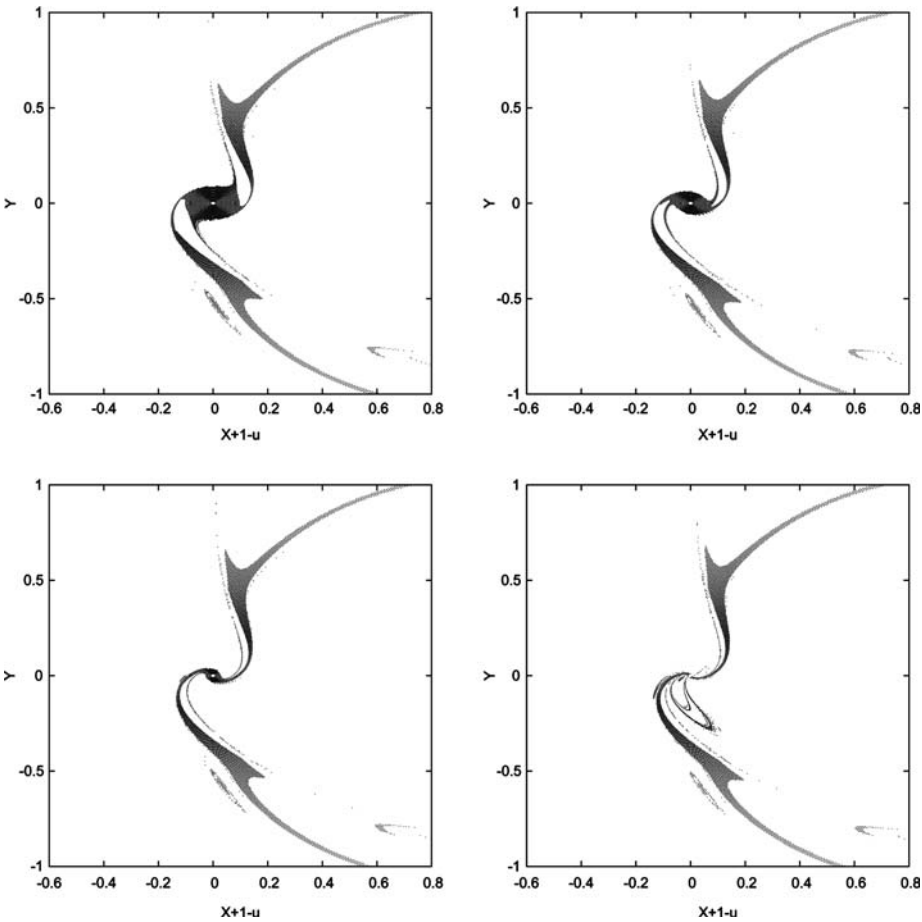

Fig. 1 From top to bottom and left to right, stable regions for initial conditions with positive velocity and eccentricities $e = 0.00$, 0.30, 0.60 and 0.90. The origin of the reference system has been set at the small primary m_2

the orbit, we have considered the possibility of having more intersections and studied how $\overline{\mathcal{W}}$ changes when we increase this number. In this way, we can define $\overline{\mathcal{W}}_n$ where the subindex n denotes the number of revolutions around m_2 taken in the stability definition. It is easy to verify that $\overline{\mathcal{W}}_n \subset \overline{\mathcal{W}}_m$ if $m < n$.

Figure 3 shows the evolution of the stable regions for $e = 0$ with n. As it has been said, as n increases the size of the stable domain decreases in the two cases under consideration (initial conditions with positive and negative velocity), but there seems to exist a rather "stable" limit for the stable regions. The evolution for other values of the eccentricity is similar.

3 Rough estimation of the stable zones

Using Jacobi's first integral, is possible to give an a-priori estimation of the lower and upper limits of the values of r_2 that produce stable motions, as will be shown in this

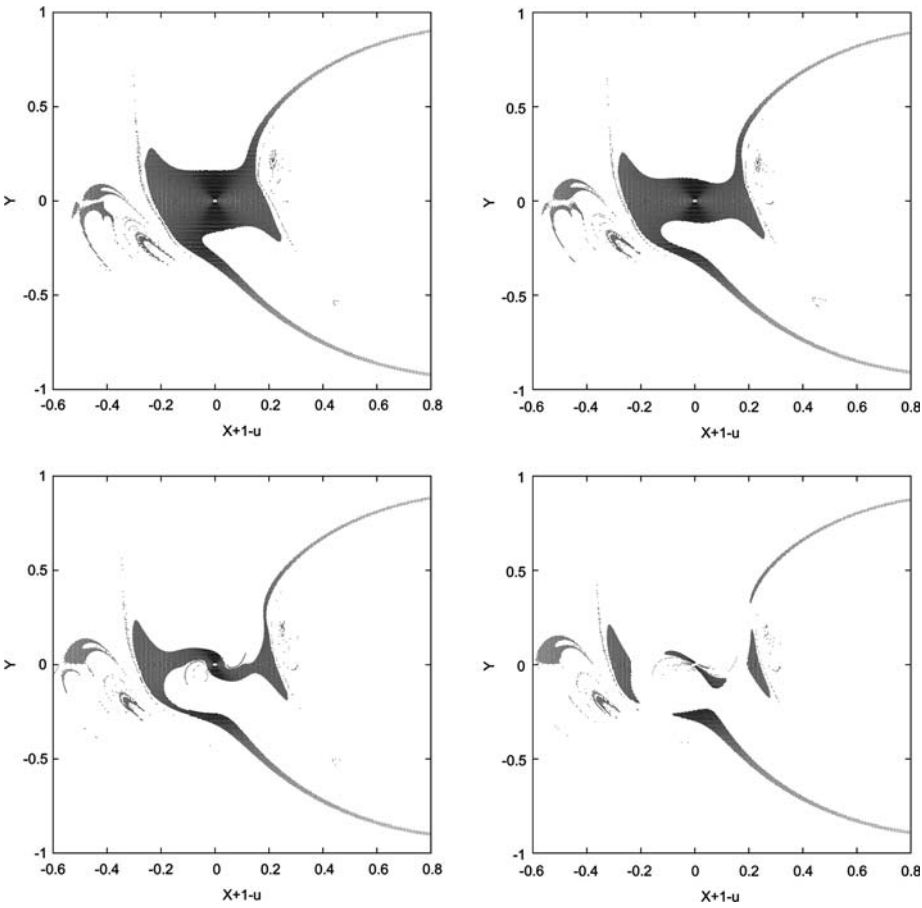

Fig. 2 From top to bottom and left to right, stable regions for initial conditions with negative velocity and eccentricities $e = 0.00, 0.30, 0.60$ and 0.90. The origin of the reference system has been set at the small primary m_2

section. The computation follows the ideas given in Belbruno (2002) and correct some errors of the formulae of this last paper. In this way, we can compare the resulting bounds with the numerical results of the preceding section.

With the initial conditions used in the algorithmic definition of the WSB, Jacobi's first integral (5) can be written as the function of e, θ and r_2 given by

$$C(r_2,\theta,e) = 2\sqrt{\mu(1+e)r_2} - r_2^2 - \frac{\mu(e-1)}{r_2} + \frac{2(1-\mu)}{\sqrt{(r_2\cos\theta - 1)^2 + r_2^2\sin^2\theta}} + (r_2\cos\theta - 1 + \mu)^2 + r_2^2\sin^2\theta + \mu(1-\mu). \quad (6)$$

This expression is independent of the two different kinds of initial conditions used. Clearly, Eq. 6 verifies the symmetry $C(r_2,\theta,e) = C(r_2,2\pi-\theta,e)$, so we will only consider values of θ in $[0,\pi]$.

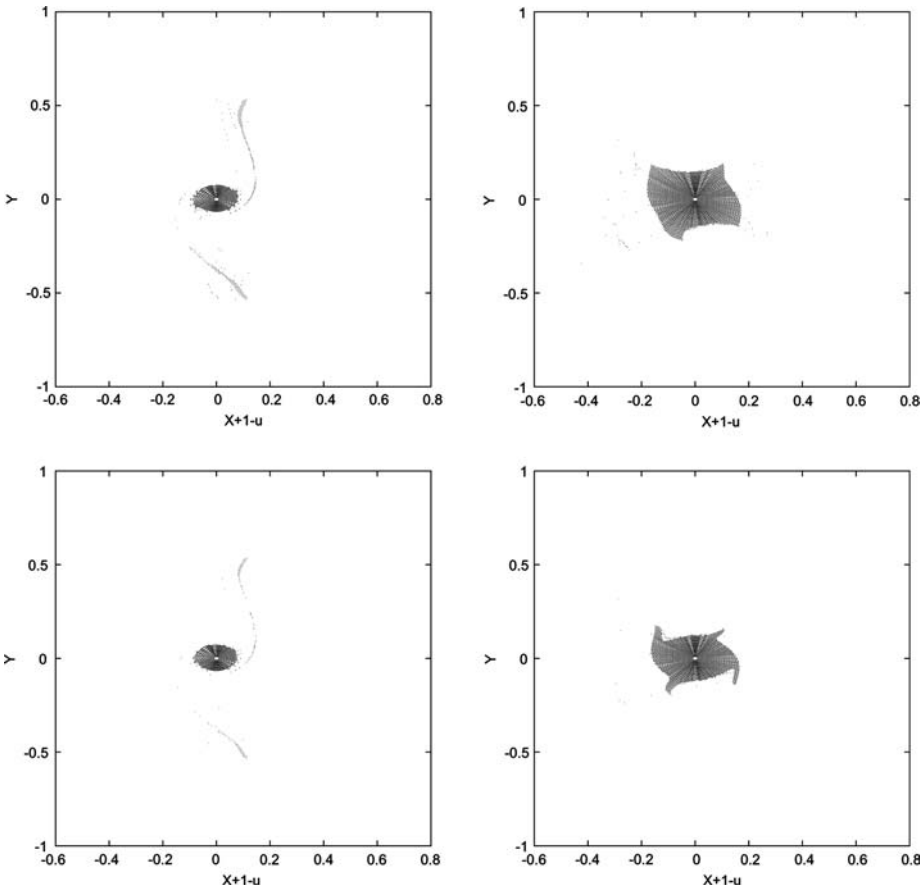

Fig. 3 Stable regions for initial conditions with positive (left column) and negative (right column) velocity and $e = 0$ when the number of intersections with l is equal to n =3 and 6. The origin of the reference system has been set at the small primary m_2

Since motions starting in a neighbourhood of m_2 can also go around m_1, the value of the Jacobi constant must be below the value corresponding to the L_2 equilibrium point—the one between both primaries—$C_2 = 3.2003449097....$ (for the Earth–Moon system), according to the behaviour of the zero-velocity curves (see Szebehely 1967). Is by this reason that the surfaces $C(r_2, \theta, e)$ must be considered only for values of $C \leq C_2$.

The intersection of the $C(r_2, \theta, e)$ surfaces with the $C = C_2$ plane is shown in Fig. 4, where it appears as two curves, $r_2^l(e)$ and $r_2^u(e)$, giving, for a fixed value of e, the lower and upper limit of the periapsis distance r_2 of the stable motions. As it can be seen from the figures, in which the stable points have been represented as dark points, the $r_2^l(e)$ can be taken as a good lower bound, but $r_2^u(e)$ is too pessimistic. In all the cases, when the eccentricity goes to 1, the value of the lower limit $r_2^l(e)$ decreases towards 0 and for all the values of θ the stable region is larger for the negative values of the velocity than for the positive ones. This is also clear in Figs. 1, 2 and 3.

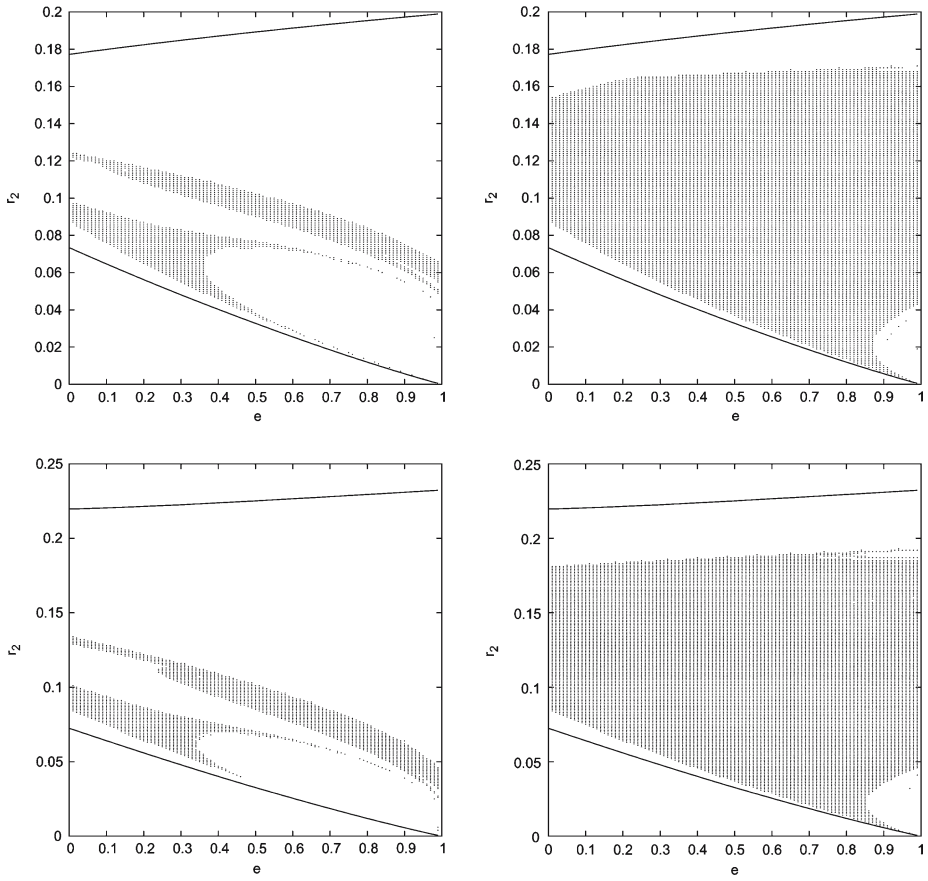

Fig. 4 Projection on the (e, r_2) plane of the stable points for $\theta = 0$ and π (the left column corresponds to points with positive velocity and the right column to points with negative velocity). The lower and upper curves in each figure are the intersections of the $C(r_2, \theta, e)$ surface with the $C = C_2$ plane

4 The role of the invariant manifolds

In this section, the connection between stable regions and the invariant manifolds associated to the central manifolds of the collinear libration points will be shown.

For a certain value of the Jacobi constant, we compute first the periodic orbits around the equilibrium points L_1 and L_2 of the Lyapunov families of planar orbits around these points, as well as the stable and unstable manifolds associated to them. On the energy level defined by the value of the Jacobi constant selected, we compute the set of stable points, according to the algorithmic definition of stability previously given. Finally we show that the invariant manifolds act as the boundary of the set of stable points.

4.1 The stable set $\overline{\mathcal{W}}(C^*)$

For illustration purposes, it is convenient to select an energy level with a large region of stable points; this happens, for instance, for the value of the Jacobi constant

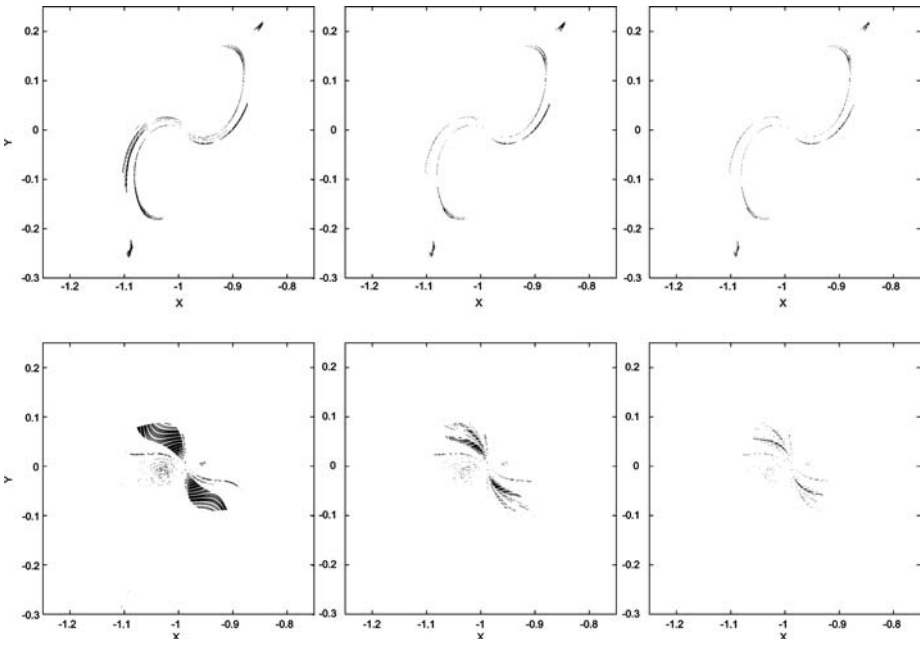

Fig. 5 (x, y)-projections of the stable regions $\overline{\mathcal{W}}_n$ for initial conditions with $C^* = 3.09998$ when the number n of intersections with l is equal to $n = 2, 4, 8$ (from left to right) . The first row shows the stable regions corresponding to positive velocity and the second row to negative velocity

$C^* = 3.09998$. For this value of C, the sets of stable points, $\overline{\mathcal{W}}_n$, $n = 2, 4, 8$ are shown in Fig. 5. For each sign of the velocity, the three sets are rather similar in shape, although $\overline{\mathcal{W}}_2$ has about five times more points than $\overline{\mathcal{W}}_8$.

From now on, we will only show the results corresponding to this value of the Jacobi constant, for other values the results are similar. Of course, since we fix the value of C, the points of this set of stable points have different values of e and θ.

4.2 Periodic orbits around L_1 and L_2

Once the energy level, C^*, has been fixed, the next step is the computation of the two planar Lyapunov periodic orbits around the libration points L_1 and L_2, respectively, with the same value of the Jacobi constant C^*. This is done using a standard predictor–corrector procedure that uses as initial approximation the orbit given by the linearised equations. The initial values of x_0 and $\dot{y_0}$ for these two periodic orbits are given in Table 1, since the orbit are symmetric with respect to the x-axis, the initial values y_0 and $\dot{x}_0$ are both zero.

Once the periodic orbits have been computed, with the help of the monodromy matrices we determine their invariant stable and unstable manifolds as follows, see Gómez et al. (2001a). Let λ be the eigenvalue of one monodromy matrix greater than one and $u(0)$ the corresponding eigenvector. If ϕ_t denotes the flow associated to the differential equations of motion (4), the differential of the flow given by the variational equations, $D\phi_t$, gives the image of $u(0)$ under the variational flow, $u(t) = D\phi_t \cdot u(0)$, for $t \in [0, T]$, where T is the period of the periodic orbit. At each point of the orbit,

Table 1 Initial conditions of the Lyapunov periodic orbits around L_1 and L_2

	x_0	$\dot{y_0}$
L_1	–1.071779887105674	–0.415925464334357
L_2	–0.900098585072386	0.406056177805114

the vector $u(t)$ together with the vector tangent to the orbit, span a plane tangent to the local unstable manifold. By forward integration of the points on this linear approximation of the manifold, we can produce the full unstable manifold.

Analogously, using the eigenvector associated to the eigenvalue smaller than one, and integrating backwards in time, we can produce the stable manifold. In fact, due to the symmetries of the equations, if the unstable eigenvector is $u(0) = (u^1(0), u^2(0), u^3(0), u^4(0))$, then the stable eigenvector is $(u^1(0), -u^2(0), -u^3(0), u^4(0))$.

Of each manifold, we will consider their positive and negative branches. This is, if $\gamma(t)$ denotes the point of the periodic orbit at which $u(t)$ is computed, the unstable manifold is globalised taking initial conditions of the form

$$\gamma(t) \pm \epsilon u(t),$$

where ϵ is a positive small number (since we are using the linear approximation of the manifold) and the $\pm$ sign defines the positive and negative branches, respectively. In our computations we have used typically a value of $\epsilon = 10^{-8}$ and the unstable eigenvector u has been computed using the power method (see Hämmerlin and Hoffmann 1990). The two branches of the unstable manifolds will be denoted by $U^+_{L_i}$, $U^-_{L_i}$ and those of the stable manifold by $S^+_{L_i}$, $S^-_{L_i}$, for $i = 1, 2$.

4.3 Selection of a suitable subset of points of the invariant manifolds

Since we want to relate invariant manifolds with the set of stable points already computed, from the 2-dimensional invariant manifolds we select those points satisfying the following two conditions:

1. The position vector, with respect to the small primary m_2 is orthogonal to the velocity vector. This is

   $$|X\dot{X} + Y\dot{Y}| < \delta,$$

   where $(X, Y, \dot{X}, \dot{Y})$ are the coordinates of the point of the manifold in a Moon-centred reference frame and δ is a tolerance which, in our computations, has been taken equal to 10^{-4}.
2. Since we want to be near the stable points computed, we only consider those points within the domain

   $$K = \{(x, y, \dot{x}, \dot{y})\,;\, x \in [-1.5, -0.5], y \in [-0.4, 0.4], \dot{x} \in [-3, 3], \dot{y} \in [-3, 3]\}.$$

If $U^+_{L_i}$, $U^-_{L_i}$, $S^+_{L_i}$, $S^-_{L_i}$, denote the different branches of the manifolds associated to the periodic orbits around L_i, for $i = 1, 2$, the points on these branches fulfiling the above two conditions will be denoted by

$$\overline{U}^+_{L_i},\ \overline{U}^-_{L_i},\ \overline{S}^+_{L_i},\ \overline{S}^-_{L_i},\ i = 1, 2.$$

To get these sets we have integrated 25,000 orbits on each branch of the invariant manifolds of the two periodic orbits, during 4π adimensional time units. This is, if $\gamma(0)$ is the initial condition of one of the periodic orbits, with period T, and $u(0)$ is associated unstable eigenvector, to produce the two branches of the unstable manifold of this orbit, we have integrated the following set of initial conditions

$$\phi_{t_i}(\gamma(0)) \pm \epsilon\, D\phi_{t_i}\,(u(0)),$$

for $t_i = i\ \Delta t$, $\Delta t = T/25000$ and $i = 0, \ldots, 24999$.

If we put together the branches of the two periodic orbits, this is, we consider

$$\overline{S} = \bigcup_{i=1,2} (\overline{S}^{+}_{L_i} \cup \overline{S}^{-}_{L_i}), \quad \overline{U} = \bigcup_{i=1,2} (\overline{U}^{+}_{L_i} \cup \overline{U}^{-}_{L_i}),$$

the set of points that are obtained are shown in Fig. 6.

Figure 7 shows that the stable sets, $\overline{\mathcal{W}}_n(C^*)$, that define the WSB verify the following inclusion: denoting by $\partial(\overline{\mathcal{W}}_n(C^*))$ the boundary of the set $\overline{\mathcal{W}}_n(C^*)$, then

$$\partial(\overline{\mathcal{W}}_n(C^*)) \subset \overline{\overline{S}}, \tag{7}$$

where $\overline{\overline{S}}$ stands for the clausure of $\overline{S}$.

To get an estimate of the inclusion given by (7) and check the coherence of the results with the tolerances used for the computations, we have done the following computation. For every point $p \in \overline{\mathcal{W}}_n(C^*)$ we have found the closest point $p^* \in \overline{S}$ and computed the distance between both. In this way, we can determine

$$d^m(n) = \min_{p \in \overline{\mathcal{W}}_n(C^*)} \left(\min_{p^* \in \overline{S}} ||p - p^*||_\infty \right),$$

$$d^M(n) = \max_{p \in \overline{\mathcal{W}}_n(C^*)} \left(\min_{p^* \in \overline{S}} ||p - p^*||_\infty \right).$$

The first of these quantities must be of the order of the maximum of the two tolerances: for the scalar product used in the definition of the $\overline{S}^{\pm}_{L_i}$ set and for the value of the Jacobi

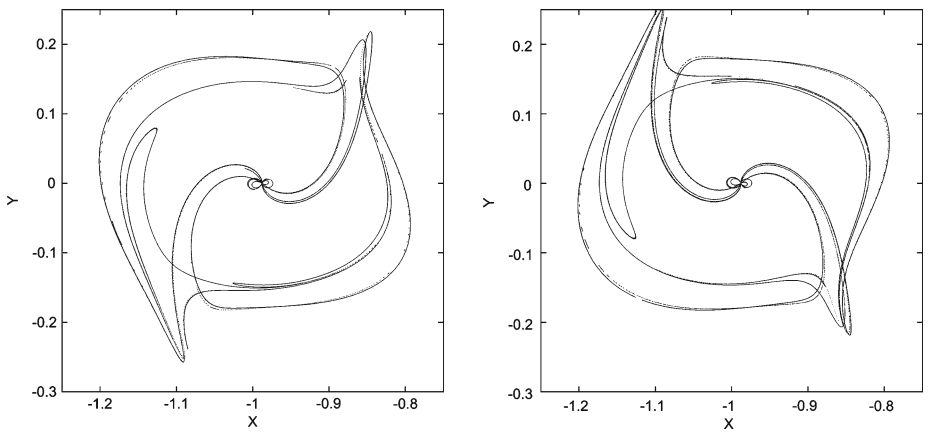

Fig. 6 Projections of the sets $\overline{S}$ and $\overline{U}$ on to the position space

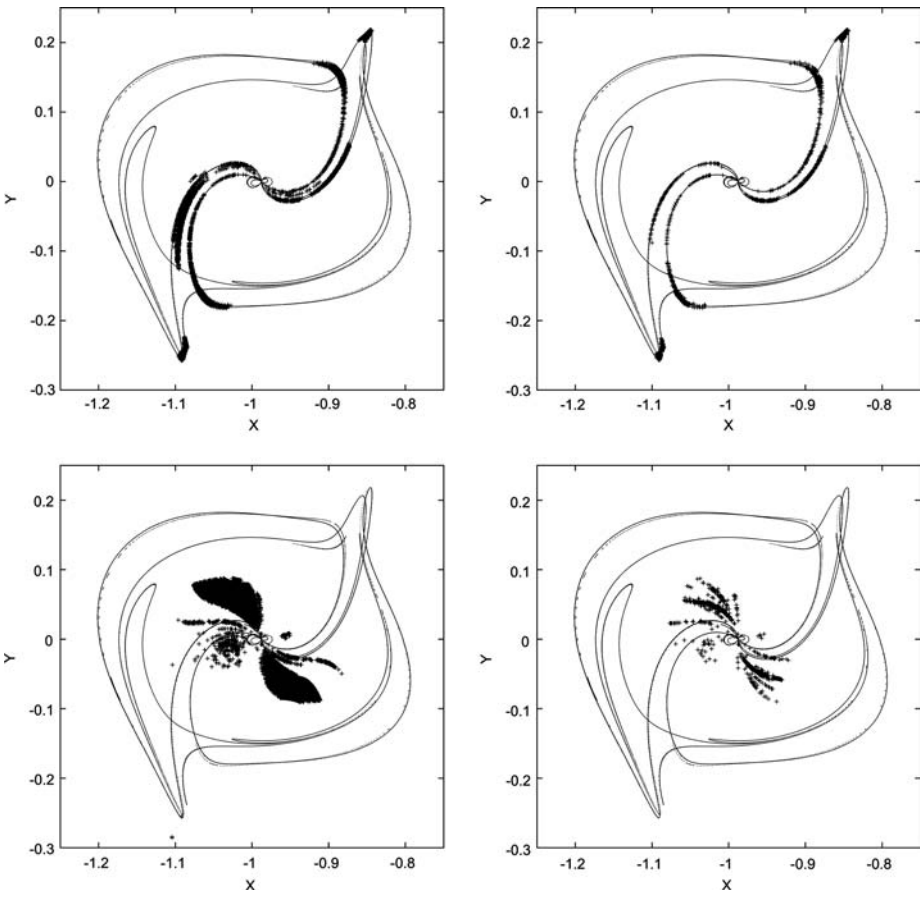

Fig. 7 Projections of the sets of stable points, with positive initial velocity, $\overline{\mathcal{W}}_n(C^*)$, for $n = 2$ (left), 8 (right) and the set $\overline{S}$ on to the position space. The first row corresponds to stable points with positive initial velocity and the second row to negative initial velocity

constant after the propagation of the initial conditions on the linear approximations of the invariant manifolds so, at most, it must be equal to $\delta = 10^{-4}$. This is what has been found, furthermore, the values of $d^m(n)$ and $d^M(n)$ become almost constant for $n > 5$.

5 Conclusions and further work

In this paper we have computed, for the RTBP, some stable regions around the small primary with a complicated boundary. We give numerical evidence that these regions seem to be bounded by the stable manifolds of the central objects around L_1 and L_2 at the same energy level. The geometry of the manifolds provide a Cantorian structure to the boundary of the stable regions. This boundary structure is similar to the one found for the stable points around the triangular libration points and the invariant manifolds of the colinear libration point L_3, see Gómez et al. (2001b). Some rough estimates of these regions can also be obtained using Jacobi's first integral.

Aside from a trivial extension to other values of the mass ratio (of interest in practical applications), we think that the next step should be to perform the extension of the study to both the spatial RTBP and some restricted four body model in order to clarify and give numerical evidence of the connection between these stable/unstable regions with the low energy transfers.

Acknowledgements The second author has been been partially supported by grants CIRIT 2001SGR-70, 2003XT-00021 (Catalonia) and BFM2003-09504 (MCYT, Spain).

References

Belbruno, E.A.: Lunar capture orbits, a method for constructing Earth–Moon trajectories and the lunar GAS mission. Proceedings of AIAA/DGLR/JSASS Inter. Propl. Conf. AIAA paper No. 87-1054 (1987)

Belbruno, E.A., Miler, J.K.: A ballistic lunar capture trajectory for the Japanese spacecraft hiten. Jet Propulsion Laboratory, IOM 312/90.4–1371-EAB (1990)

Belbruno, E.A.: The dynamical mechanism of ballistic lunar capture transfers in the four body problem from the perspective of invariant manifolds and hill's regions. Institut d'Estudis Catalans, CRM Preprint No. 270, Barcelona (1994)

Belbruno, E.A., Humble R., Coil, J.: Ballistic capture lunar transfer determination for the U.S. Air Force Academy Blue Moon Mission. AAS/AIAA Spaceflight Mechanics Meeting, Paper No. AAS 96-171 (1997)

Belbruno, E.A., Carrico, J.P.: Calculation of weak stability boundary ballistic lunar transfer trajectories. AIAA/AAS Astrodynamics Specialist Conference, Paper No. AIAA 2000–4142 (2000)

Belbruno, E.A.: Analytic estimation of weak stability boundaries and low energy transfers. Contemp Math **292**, 17–45 (2002)

Belbruno, E.A.: (2004) Capture Dynamics and Chaotic Motions in Celestial Mechanics. Princeton University Press, Princeton, NI (2004)

Belló, M., Graziani, F., Teofilato, P., Circi, C., Porfilio, M. Hechler, M.: A systematic analysis on weak stability boundary transfers to the moon. 51st International Astronautical Congress, Paper No. IAF–00-A.6.03 (2000)

Biesbroek, R.: Study on lunar trajectories from GTO by using weak stability boundary transfers and swing-by's. European Space Agency, ESTEC working paper No. 2014 (1997)

Circi, C., Teofilato, P.: On the dynamics of weak stability boundary lunar transfers. Celestial Mech. Dyn. Astron. **79**, 41–72 (2001)

Gómez, G., Llibre, J., Matínez, R., Simó, C.: Dynamics and Mission Design Near Libration Point Orbits—Volume I: Fundamentals: The Case of Collinear Libration Points. World Scientific, Singapore (2001a)

Gómez, G., Jorba, À., Masdemont, J., Simó, C.: Dynamics and Mission Design Near Libration Point Orbits—Volume IV: Advanced Methods for Triangular Points. World Scientific, Singapore (2001b)

Hämmerlin, C., Hoffmann, K.H.: Numerical Mathematics. Springer, Berlin (1990)

Koon, W.S., Lo, M.W., Marsden, J.E., Ross, S.D.: Shoot the moon. AAS/AIAA Space Flight Mechanics Meeting, Paper No. AAS 00-166 (2000)

Koon, W.S., Lo, M.W., Marsden, J.E., Ross, S.D.: Low energy transfer to the moon. Celestial Mech. Dyn. Astron. **81**, 63–73 (2001)

Miller, J.K., Belbruno, E.A.: A method for the construction of a lunar transfer trajectory using ballistic capture. AAS/AIAA Spaceflight Mechanics Meeting, Paper No. AAS 91-100 (1991)

Pollard, H.: Mathematical Introduction to Celestial Mechanics. Prentice Hall, Englewood Cliffs, NJ (1996)

Szebehely, V.: Theory of Orbits. Academic Press, New york (1967)

Yagasaki, K.: Sun-perturbed Earth-to-Moon transfers with low energy and moderate flight time. Celestial Mech. Dyn. Astron. **90**, 197–212 (2004a)

Yagasaki, K.: Computation of low energy Earth-to-Moon transfers with moderate flight time. Physica D **197**, 313–331 (2004b)